

Supporting Information -

**Phonon scattering through a local anisotropic
structural disorder in the thermoelectric solid
solution $\text{Cu}_2\text{Zn}_{1-x}\text{Fe}_x\text{GeSe}_4$.**

Wolfgang G. Zeier,^{†,‡} Yanzhong Pei,[‡] Gregory Pomrehn,[‡] Tristan Day,[‡] Nicholas
Heinz,[‡] Christophe P. Heinrich,[†] G. Jeffrey Snyder,^{*,‡} and Wolfgang Tremel^{*,†}

*Institut für Anorganische Chemie und Analytische Chemie der Johannes Gutenberg-Universität,
Duesbergweg 10-14, D-55099 Mainz, and Material Science, California Institute of Technology,
Pasadena, CA, USA*

E-mail: jsnyder@caltech.edu; tremel@uni-mainz.de

^{*}To whom correspondence should be addressed

[†]Institut für Anorganische Chemie und Analytische Chemie der Johannes Gutenberg-Universität

[‡]Material Science, California Institute of Technology

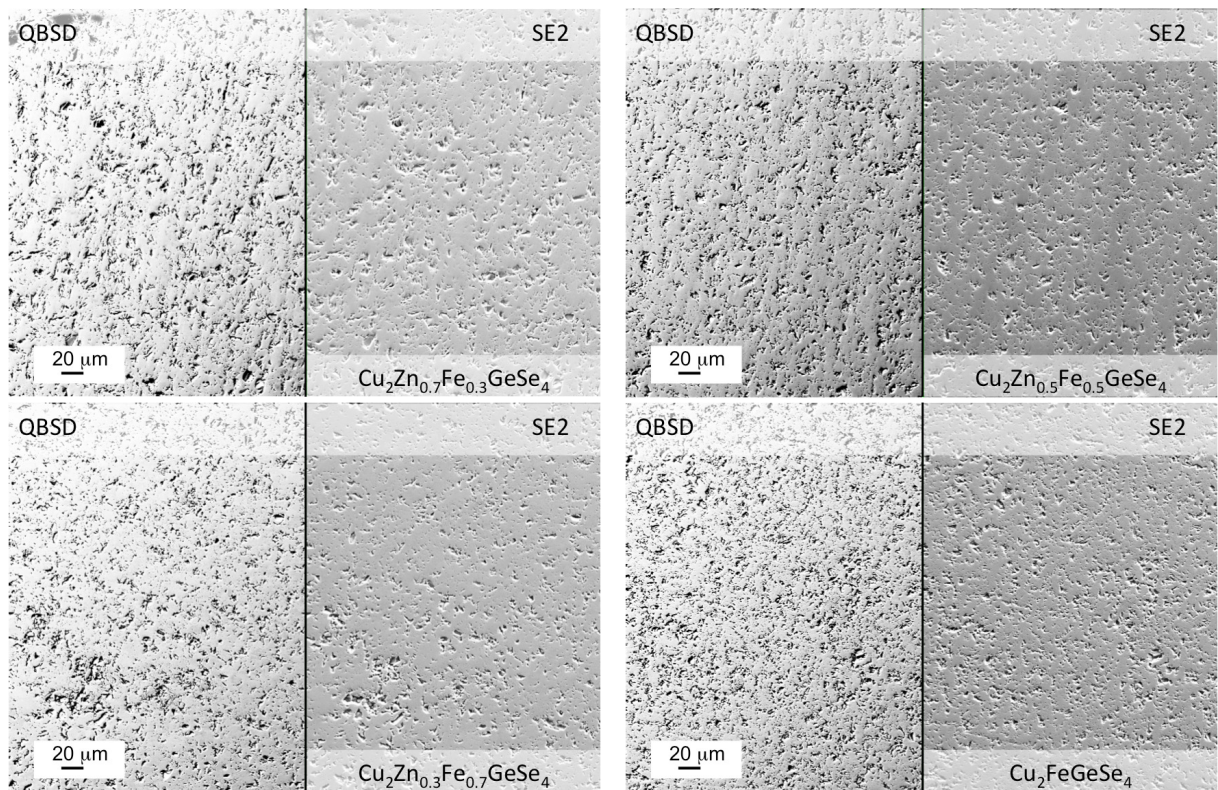


Figure S 1: SEM micrographs of $\text{Cu}_2\text{Zn}_{1-x}\text{Fe}_x\text{GeSe}_4$ in backscattered (QBSD) and secondary electron mode (SE2), showing dense materials with similar microstructures and grain sizes between 10-20 μm .

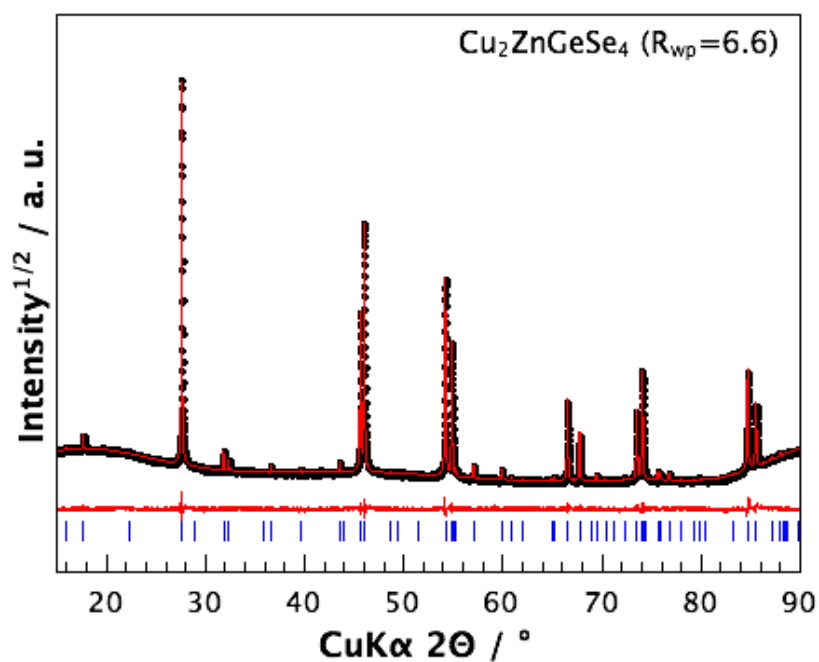


Figure S 2: X-ray diffraction data including profile fit, profile difference, and profile residuals of the corresponding Rietveld fit of phase pure Cu₂ZnGeSe₄.

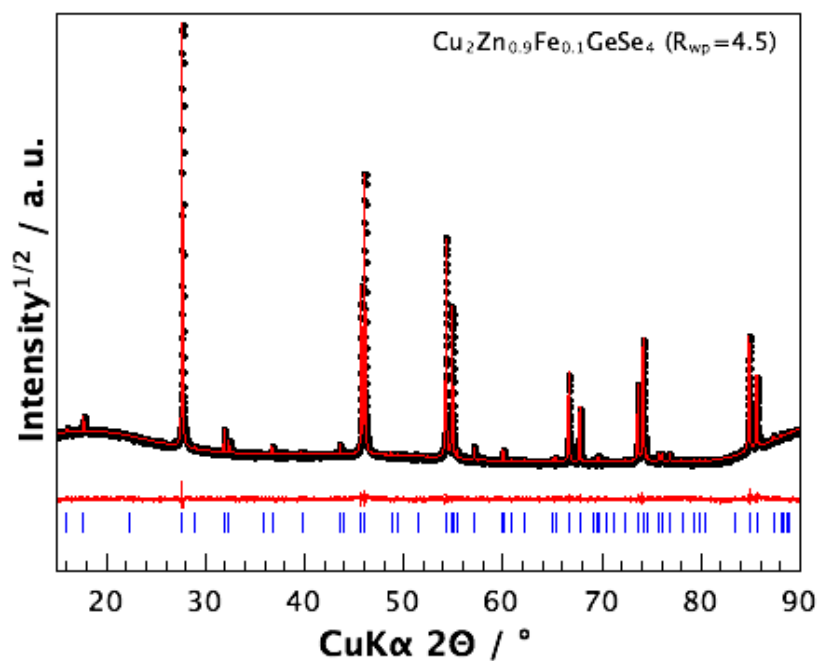


Figure S 3: X-ray diffraction data including profile fit, profile difference, and profile residuals of the corresponding Pawley fit of phase pure Cu₂Zn_{1-x}Fe_xGeSe₄.

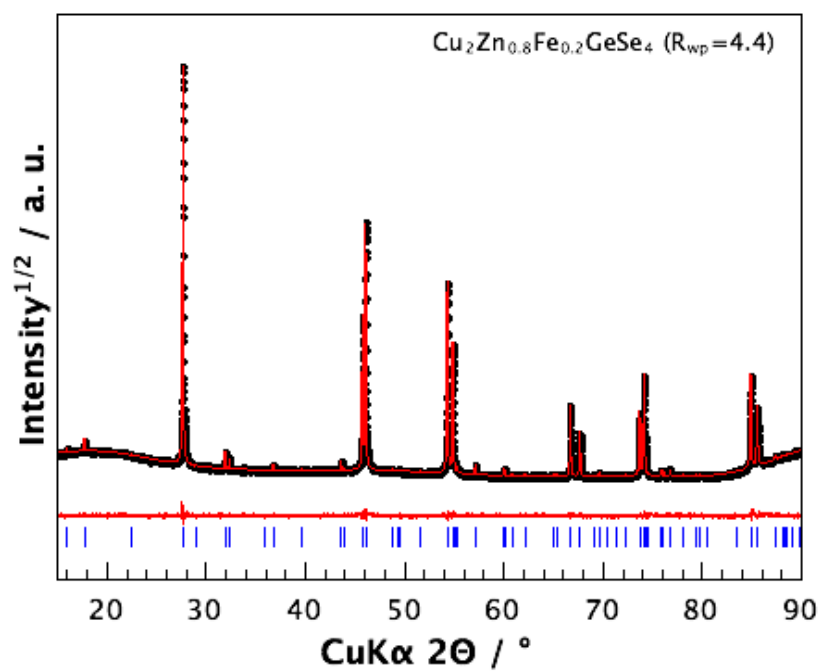


Figure S 4: X-ray diffraction data including profile fit, profile difference, and profile residuals of the corresponding Pawley fit of phase pure $\text{Cu}_2\text{Zn}_{1-x}\text{Fe}_x\text{GeSe}_4$.

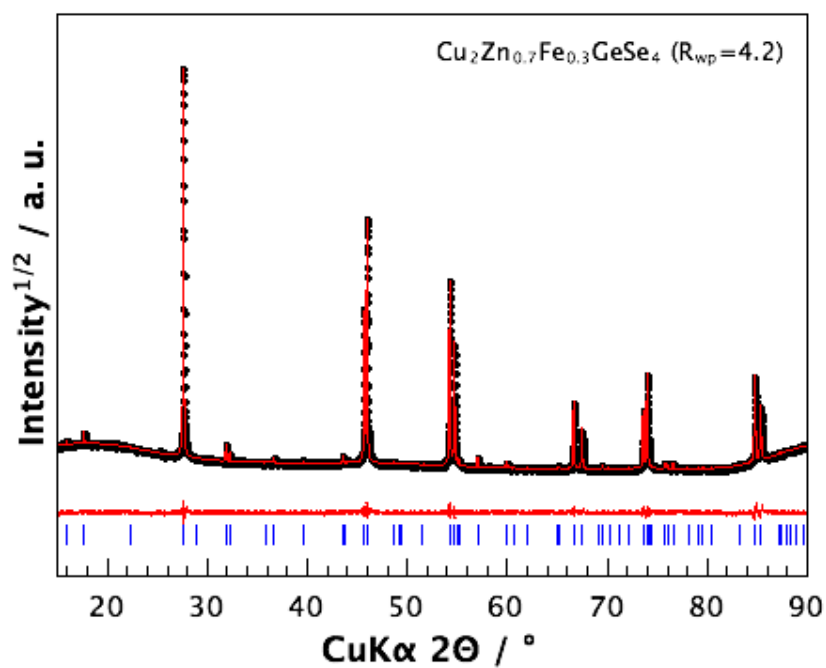


Figure S 5: X-ray diffraction data including profile fit, profile difference, and profile residuals of the corresponding Pawley fit of phase pure $\text{Cu}_2\text{Zn}_{1-x}\text{Fe}_x\text{GeSe}_4$.

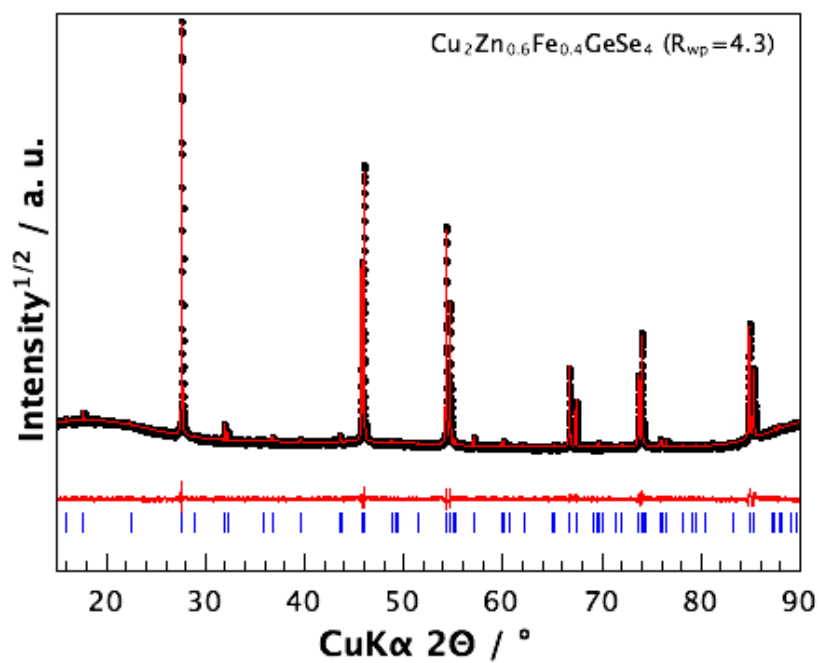


Figure S 6: X-ray diffraction data including profile fit, profile difference, and profile residuals of the corresponding Pawley fit of phase pure $\text{Cu}_2\text{Zn}_{1-x}\text{Fe}_x\text{GeSe}_4$.

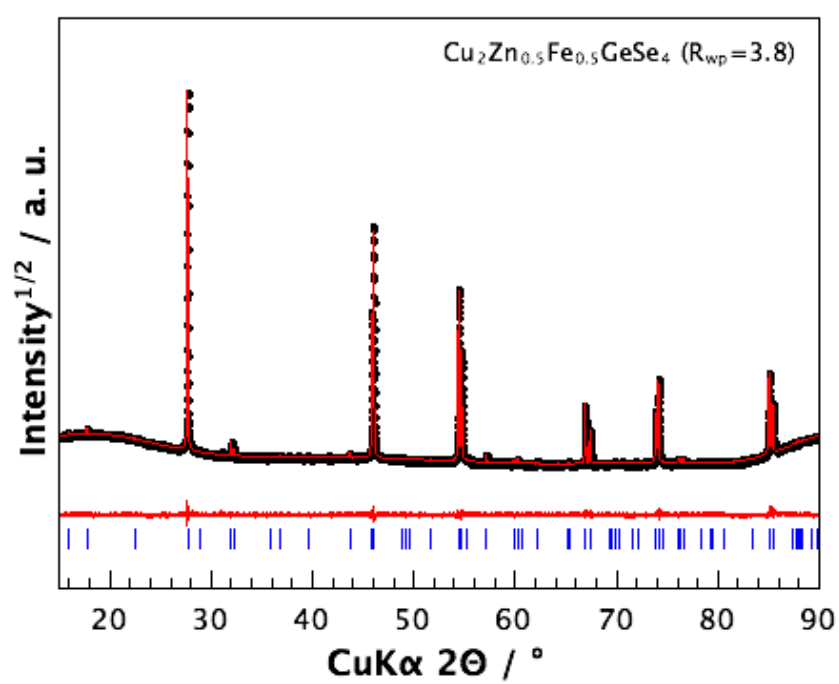


Figure S 7: X-ray diffraction data including profile fit, profile difference, and profile residuals of the corresponding Pawley fit of phase pure $\text{Cu}_2\text{Zn}_{1-x}\text{Fe}_x\text{GeSe}_4$.

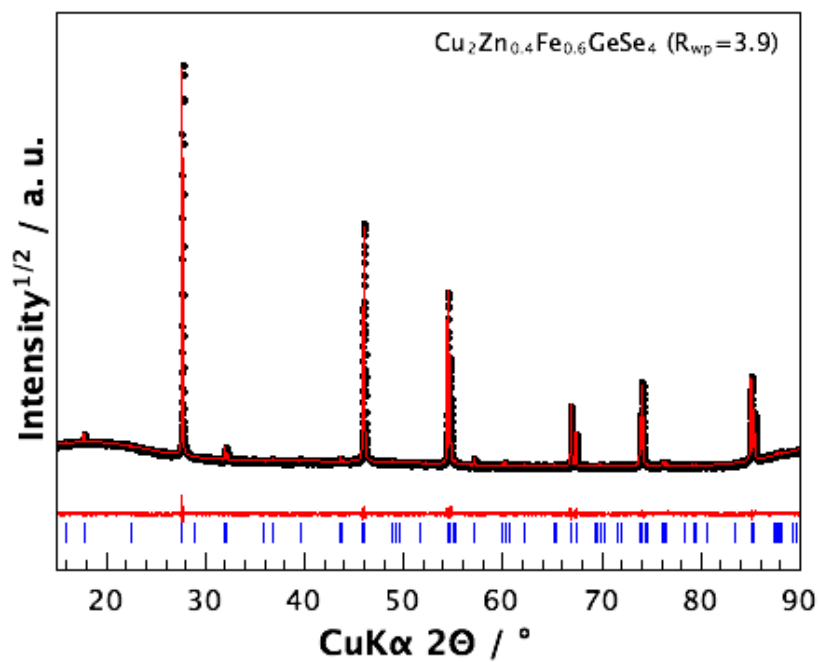


Figure S 8: X-ray diffraction data including profile fit, profile difference, and profile residuals of the corresponding Pawley fit of phase pure $\text{Cu}_2\text{Zn}_{1-x}\text{Fe}_x\text{GeSe}_4$.

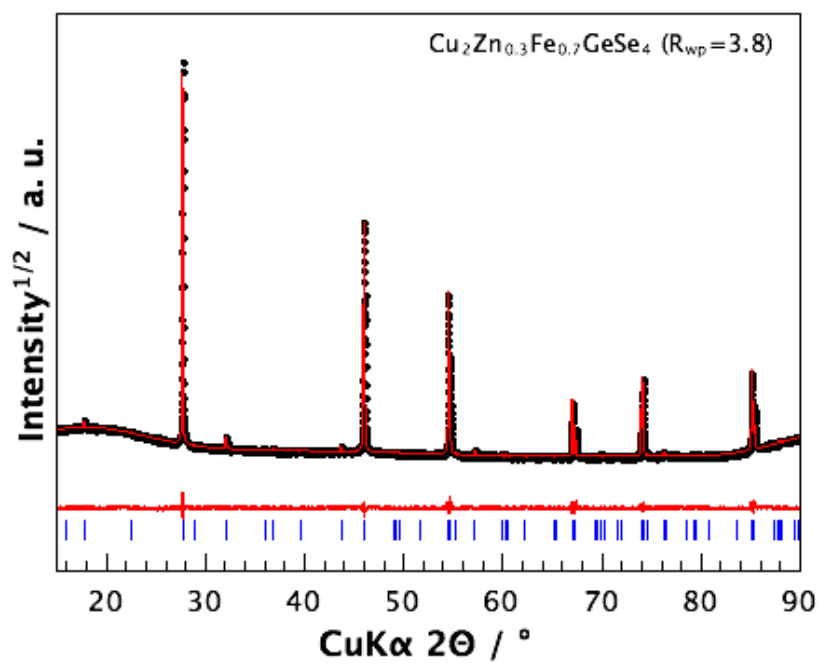


Figure S 9: X-ray diffraction data including profile fit, profile difference, and profile residuals of the corresponding Pawley fit of phase pure $\text{Cu}_2\text{Zn}_{1-x}\text{Fe}_x\text{GeSe}_4$.

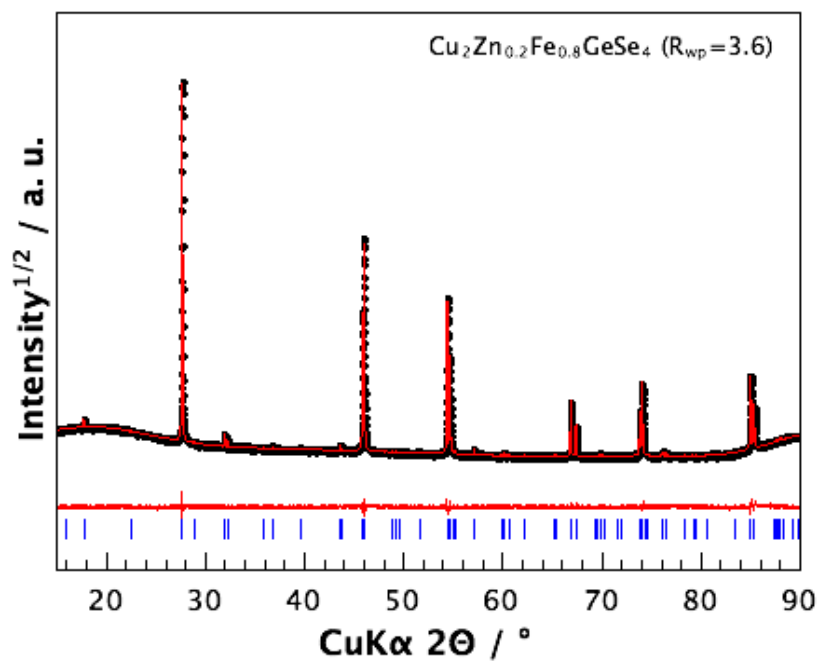


Figure S 10: X-ray diffraction data including profile fit, profile difference, and profile residuals of phase pure $\text{Cu}_2\text{Zn}_{1-x}\text{Fe}_x\text{GeSe}_4$.

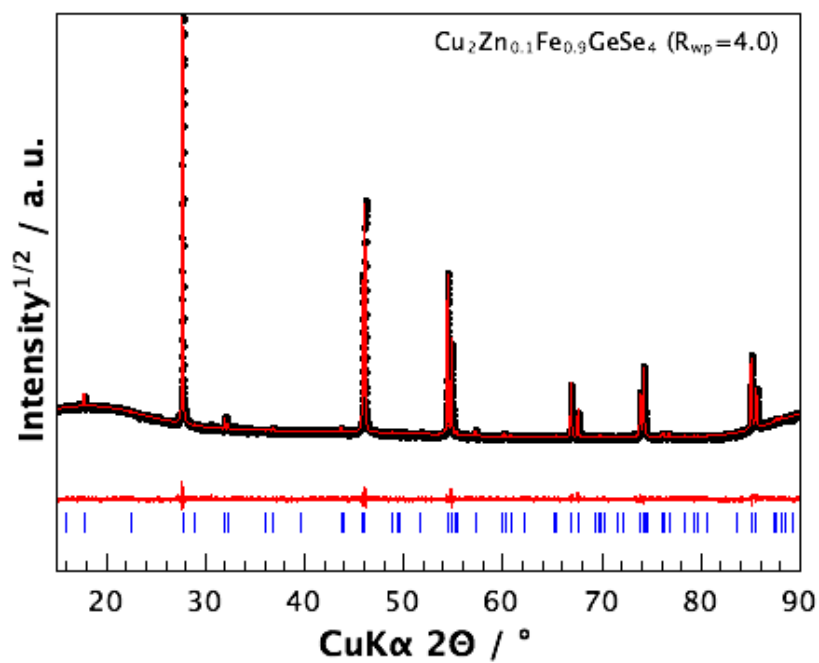


Figure S 11: X-ray diffraction data including profile fit, profile difference, and profile residuals of phase pure $\text{Cu}_2\text{Zn}_{1-x}\text{Fe}_x\text{GeSe}_4$.

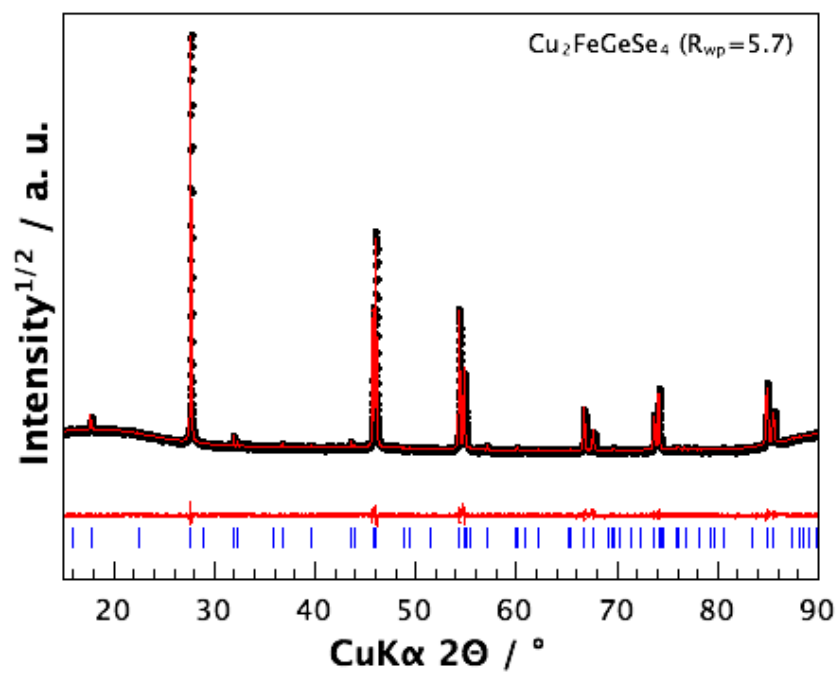


Figure S 12: X-ray diffraction data including profile fit, profile difference, and profile residuals of phase pure $\text{Cu}_2\text{Zn}_{1-x}\text{Fe}_x\text{GeSe}_4$.